ENVIRONMENTAL RESEARCHCLIMATE



LETTER • OPEN ACCESS

Sea ice feedbacks cause more greenhouse cooling than greenhouse warming at high northern latitudes on multi-century timescales

To cite this article: Jennifer E Kay et al 2024 Environ. Res.: Climate 3 041003

View the article online for updates and enhancements.

You may also like

- Net evaporation-induced mangrove area loss across low-lying Caribbean islands Isamar M Cortés, Jorge Lorenzo-Trueba, Andre S Rovai et al.
- Broadening the scope of anthropogenic influence in extreme event attribution Aglaé Jézéquel, Ana Bastos, Davide Faranda et al.
- Understanding the response of tropical overturning circulations to greenhouse gas and aerosol forcing
 Vishisth Kalik, R Krishnan, D C Ayantika et al

ENVIRONMENTAL RESEARCH

CLIMATE



OPEN ACCESS

RECEIVED

16 April 2024

REVISED

10 September 2024

ACCEPTED FOR PUBLICATION 26 September 2024

PUBLISHED 8 October 2024

Original content from this work may be used under the terms of the Creative Commons Attribution 4.0 licence.

Any further distribution of this work must maintain attribution to the author(s) and the title of the work, journal citation and DOI.



LETTER

Sea ice feedbacks cause more greenhouse cooling than greenhouse warming at high northern latitudes on multi-century timescales

Jennifer E Kay^{1,2,∗}, Yu-Chiao Liang³, Shih-Ni Zhou³, and Nicola Maher⁴,

- Department of Atmospheric and Oceanic Sciences, University of Colorado Boulder, Boulder, CO, United States of America
- ² Cooperative Institute for Research in Environmental Sciences, University of Colorado Boulder, Boulder, CO, United States of America
- ³ Department of Atmospheric Sciences, National Taiwan University, Taipei, Taiwan
- ⁴ ARC Centre of Excellence for Climate Extremes and Research School of Earth Sciences Australian National University, Canberra, Australian Capital Territory, Australia
- * Author to whom any correspondence should be addressed.

E-mail: Jennifer.E.Kay@colorado.edu

Keywords: feedbacks, sea ice, greenhouse cooling, greenhouse warming

Supplementary material for this article is available online

Abstract

In contrast to surface greenhouse warming, surface greenhouse cooling has been less explored, especially on multi-century timescales. Here, we assess the processes controlling the pacing and magnitude of the multi-century surface temperature response to instantaneously doubling and halving atmospheric carbon dioxide concentrations in a modern global coupled climate model. Over the first decades, surface greenhouse warming is larger and faster than surface greenhouse cooling both globally and at high northern latitudes (45–90° N). Yet, this initial multi-decadal response difference does not persist. After year 150, additional surface warming is negligible, but surface cooling and sea ice expansion continues. Notably, the equilibration timescale for high northern latitude surface cooling (~437 years) is more than double the equivalent timescale for warming. The high northern latitude responses differ most at the sea ice edge. Under greenhouse cooling, the sea ice edge slowly creeps southward into the mid-latitude oceans amplified by positive lapse rate and surface albedo feedbacks. While greenhouse warming and sea ice loss at high northern latitudes occurs on multi-decadal timescales, greenhouse cooling and sea ice expansion occurs on multi-century timescales. Overall, this work shows the importance of multi-century timescales and sea ice processes for understanding high northern latitude climate responses.

1. Introduction

The climate system equilibrates to greenhouse gas forcing on centennial to millennial timescales (e.g., Stouffer 2004). Despite this well-known equilibration timescale, many model intercomparison protocols only require simulation lengths of 150 years. For example, the most recent coupled model intercomparison project (CMIP) Phase 6 (CMIP6) used 150 years of an abrupt 4xCO₂ experiment to estimate equilibrium climate sensitivity (Eyring et al 2016). Recently, millennial-length simulations from CMIP-class models have been collected to enable new insights into the climate system response to increased carbon dioxide on multi-century timescales (Rugenstein et al 2019). All models in this long run collection simulated more equilibrium global greenhouse warming by year 1000 than the equilibrium warming estimates based on the first 150 years (Rugenstein et al 2020). In addition, greenhouse warming and radiative feedback patterns evolve after 150 years. For example, Hill et al (2022) used the collection to show the anti-symmetric polar warming pattern (larger northern hemisphere response) weakens with time, but that the symmetric component of polar warming changes minimally with time.



While greenhouse warming response timescales and patterns have been studied (e.g. Stouffer 2004, Armour et al 2013, Hill et al 2022), research on corresponding greenhouse cooling timescales and the related processes is relatively rare. Two decades ago, Stouffer (2004) contrasted greenhouse cooling and warming in long runs with an early global coupled atmosphere-ocean climate model. With vertical mixing as the dominant process, surface cooling was faster than surface warming because surface ocean cooling destabilized the water column, a process also noted by Manabe et al (1991). Interestingly, Stouffer (2004) noted faster warming than cooling in the northern hemisphere near-surface ocean in their millennial timescale simulations. Indeed, the northern hemisphere surface response was almost 500 years faster for warming than for cooling. In the Pacific, this fast warming was more efficiently trapped near the surface due to reduced vertical mixing associated with surface ocean heating. The north Atlantic response was complex due to the time-evolving impacts of the meridional overturning circulation on the near-surface ocean, as also found in Stouffer and Manabe (2003). These early and more recent studies have emphasized that ocean vertical mixing is fundamental to high-northern latitude near-surface greenhouse response (e.g. Yang and Zhu 2011, Jansen et al 2018).

While pioneering work has set the stage, it is timely to revisit the processes controlling the relative pacing and magnitude of greenhouse warming and greenhouse cooling. Today's climate models have higher resolution and more complex physical representation of the coupling and feedbacks than the early model used by Stouffer (2004). In addition, climate scientists have developed tools for quantifying forcing and feedbacks that were not employed by Stouffer (2004) and other studies analyzing multi-century responses to greenhouse gases alone (e.g. Kutzbach et al 2013). Finally, recent studies have emphasized that cooling during the last glacial maximum provides a strong constraint on greenhouse warming's upper bound (e.g. Sherwood et al 2020, Zhu et al 2022). But trusting this paleoclimate constraint requires understanding the extent to which feedback magnitudes and timescales are equal-but-opposite under greenhouse warming and greenhouse cooling.

Interestingly, a renewed effort to explain climate response to a wide CO2 forcing scenarios has recently emerged. For example, Chalmers et al (2022) attributed more global 2xCO₂ warming than global 0.5xCO₂ cooling after 150 years to 2xCO₂ having larger radiative forcing and feedbacks than 0.5xCO₂. Adding emphasis to the importance of CO₂ forcing itself, Mitevski et al (2022) found that non-logarithmic CO₂ forcing explains response differences across a large range of CO2 forcing, especially at low CO2 concentrations. Focused on the Arctic (60–90° N), Zhou et al (2023) found Arctic surface temperature amplification over a large range of CO_2 concentrations (1/8x-8x pre-industrial values). Notably, the largest Arctic amplification occurred when CO₂ concentrations were reduced to an eighth, a quarter, and half of pre-industrial values. All of these aforementioned recent studies used model simulations with lengths of 150 years. Here, we ask: Do conclusions using multi-decadal experiments hold as integration lengths increase to multi-century timescales at high northern latitudes? Pertinent to this timescale question, Chalmers et al (2022) noted the surface greenhouse cooling response at high northern latitudes was slow to develop and continued to evolve throughout 150 years of simulation. This slow and continued surface cooling response was in stark contrast to a fast and largely equilibrated greenhouse warming response at high northern latitudes. Chalmers et al (2022) go further and relate these high northern latitude response timing differences to the timing of sea ice advance/retreat and associated amplifying positive lapse rate and surface albedo feedbacks.

The goals of this work are to quantify and understand the pacing of greenhouse cooling and warming on multi-century timescales, especially at high northern latitudes. Specifically, we contrast greenhouse warming and greenhouse cooling on multi-decadal and multi-century timescales. Additionally, we ask what processes explain any magnitude and pacing differences in near-surface warming and cooling at high northern latitudes. As we will show, running climate modeling experiments out 1000 years affects cooling more than warming both globally and at high northern latitudes. While northern hemisphere warming equilibrates quickly on multi-decadal timescales, northern hemisphere cooling persists on much longer multi-century timescales. In our multi-century simulations, sea ice change and associated positive feedbacks explain this warming-cooling timing asymmetry. Overall, our results emphasize the sea ice change is critical to asymmetries between warm and cool greenhouse climates on multi-century timescales.

2. Methods

We use a well-vetted and respected modern climate model: the Community Earth System Model version 1 with the Community Atmosphere Model 5 (CESM1-CAM5 Hurrell et al 2013). CESM1-CAM5 outperforms many models of its class for representing the modern observed global distributions of surface temperature and precipitation (Knutti et al 2013). We use the same code base (i.e. physics, resolution, and 1850 forcing) as



Table 1. Model runs used in this study. All runs use the Community Earth System Model version 1 Large Ensemble version (CESM1-LE, Kay *et al* 2015) at the standard one-degree horizontal resolution. The equilibration timescale (τ) was found by fitting surface temperature (TS) data over all 1000 years of the simulation to an exponential: TS(year) = aEXP(τ *year).

	Description	References	au global	τ 45–90° N	τ 70–90° N
CNT	Fully coupled 1850 control	Kay et al (2015)	n/a	n/a	n/a
2xCO ₂	Abrupt 2xCO ₂ fully coupled	Frey and Kay (2017) (years 1–150); this work (years 151–1000)	219 years.	200 years.	200 years.
0.5xCO ₂	Abrupt 0.5xCO ₂ fully coupled	Chalmers <i>et al</i> (2022) (years 1–150); this work (years 151–1000)	567 years.	437 years.	284 years.

the CESM1 large ensemble project, a project focused on quantifying internal variability and forced climate change in historical and near-future climate projections (Kay *et al* 2015).

This work benefits from simulations that have already been completed, analyzed, and published using CESM1 (table 1). Forcing, rapid adjustments, and feedbacks over first 150 years have been quantified for both $0.5xCO_2$ and $2xCO_2$ (Chalmers *et al* 2022). Notably, the radiative forcing is $\sim 10\%$ stronger for $2xCO_2$ than for $0.5xCO_2$ forcing in this model. Also useful for, Mitevski *et al* (2021), Mitevski *et al* (2022), and Zhou *et al* (2023) have analyzed the 150 year climate forcing and response over a much larger range of CO_2 forcing using this model. In addition, multi-century simulations for the last glacial maximum have been run and analyzed for this model (Zhu and Poulsen 2021).

For this work, we extend existing 150 year-long instantaneous $2xCO_2$ and $0.5xCO_2$ experiments out to 1000 years (table 1). These two simulations took over 100 d of wall clock to complete on the Cheyenne supercomputer (doi:10.5065/D6RX99HX). After 150 years, the $2xCO_2$ and $0.5xCO_2$ model runs had top-of-model energy imbalances of $\sim 1 \text{ Wm}^{-2}$ (Chalmers et al 2022). By extending out to year 1000, the top-of-model imbalances decrease to $+0.32 \text{ Wm}^{-2}$ for the $2xCO_2$ experiment and -0.38 Wm^{-2} for the $0.5xCO_2$ experiment (see supplementary figure 1). For comparison, the 1850 control simulation (CNT, table 1) is balanced at 0.2 Wm^{-2} over the 1000 years. Thus after 1000 years, the imbalances of both the $2xCO_2$ and $0.5xCO_2$ experiments are small (within 0.15 Wm^{-2} of their initial values).

We use standard methods to analyze the climate response and feedbacks after 1000 years and compare it with the response on shorter timescales. Like many climate studies (e.g. Chalmers et al 2022, Zhou et al 2023), we estimate the influence of individual climate drivers using radiative feedbacks. Specifically, we use CESM1-CAM5 radiative kernels (Pendergrass et al 2018) to calculate Planck, lapse rate, water vapor, surface albedo and cloud radiative feedback parameters. Our shortwave cloud radiative feedback calculations use the radiative kernel method, a practice that is not recommended (Chalmers et al 2022). That said, cloud feedbacks are not emphasized in this work due to well-known cloud biases in CESM1-CAM5. Most notable of these biases is a large underestimation of supercooled liquid in mixed phase clouds (e.g. Kay et al 2016, Tan et al 2016, Middlemas et al 2020) that causes an underestimation of cloud impacts on radiation at middle and high latitudes.

3. Results

3.1. Surface temperature response and its association with sea ice

We begin by assessing the time evolution of annual mean surface temperature responses to $2xCO_2$ and $0.5xCO_2$ forcing (figure 1). In the first few decades, there is more $2xCO_2$ warming than $0.5xCO_2$ cooling both globally and at high northern latitudes (herein defined as $45-90^\circ$ N). At year 150, the $2xCO_2$ global warming is 20% larger than $0.5xCO_2$ global cooling (figure 1(a), see also Chalmers et al (2022) figure 1). Also at year 150, the high northern latitude surface temperature response is similar in magnitude for $2xCO_2$ warming and $0.5xCO_2$ cooling (figure 1(a)). As a result, the high northern latitude amplification of ~ 2 is a bit larger for $0.5xCO_2$ than for $2xCO_2$ at year 150 (figure 1(b)). After year 150, $0.5xCO_2$ cooling continues and strengthens both globally and especially at high northern latitudes. In contrast, there is little additional global and high northern latitude $2xCO_2$ warming after year 150. After year 150, the $2xCO_2$ high northern latitude amplification remains constant at ~ 2 while the $0.5xCO_2$ amplification remains at ~ 2.5 .

Motivated to quantify slower 0.5xCO₂ cooling than 2xCO₂ warming both globally and at high northern latitudes (figure 1), we next compare response e-folding timescales for surface temperature (table 1). For



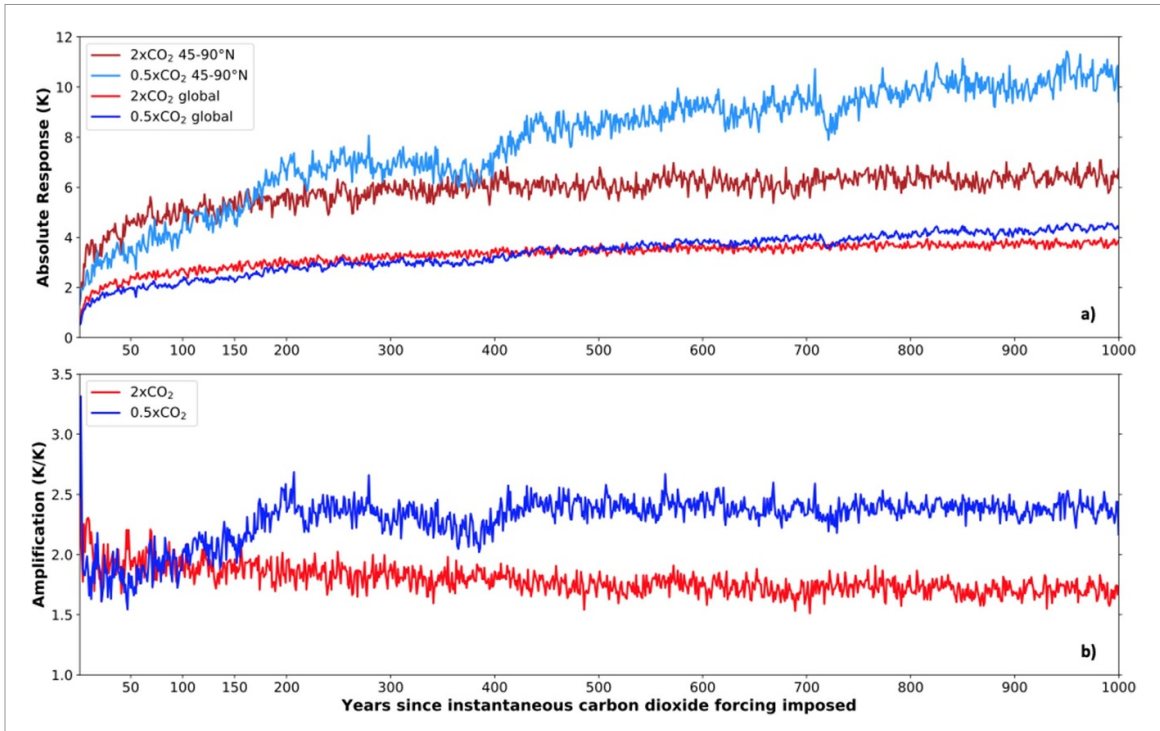


Figure 1. Time series of annual mean surface temperature responses to $2xCO_2$ and $0.5xCO_2$ instantaneous carbon dioxide forcing: (a) Global and high northern latitudes $(45–90^{\circ} \text{ N})$ absolute response; (b) Amplification, i.e. high northern latitude values divided by global values. All responses are relative to the 1850 control run (CNT years 400–1399, see table 1). For (a), absolute responses are plotted to facilitate direct comparison between the magnitude of $2xCO_2$ warming and $0.5xCO_2$ cooling.

the globe, the e-folding timescale for 0.5xCO_2 surface cooling (~ 567 years) is more than double that for 2xCO_2 surface warming (~ 219 years). At high northern latitudes ($45-90^\circ$ N), the surface temperature response timescale is also more than twice as long for 0.5xCO_2 cooling (~ 437 years) than for 2xCO_2 warming (~ 200 years). At the highest northern latitudes (i.e. $70-90^\circ$ N, a definition typically used for the modern Arctic), the 0.5xCO_2 cooling e-folding timescale decreases (~ 284 years) while the 2xCO_2 cooling e-folding timescale stays the same (still ~ 200 years).

We next examine the time-evolving zonal mean surface temperature response (figure 2) and its association with sea ice (figure 3). Notably, the zonal-time pattern of surface temperature and sea ice responses are similar, regardless of the forcing. Under $2xCO_2$, warming (figure 2(a)) and sea ice loss (figure 3(a)) maximize poleward of 70° N with the largest changes occurring in the first few decades. In contrast, high northern latitude cooling (figure 2(b)) and sea ice gain (figure 3(b)) change on multi-century timescales under $0.5xCO_2$. The $0.5xCO_2$ cooling and sea ice expansion start at the highest northern latitudes and creep southward to 45° N. By the end of the simulations at year 1000, the absolute surface temperature and sea ice response for $0.5xCO_2$ exceeds that for $2xCO_2$ poleward of 45° N for all but the very highest northern latitudes (figures 2(c) and 3(c)). These results provide an explanation for why the highest northern latitudes ($70-90^\circ$ N) have the most similar $0.5xCO_2$ and $2xCO_2$ equilibration timescales (table 1). At these highest northern latitudes, sea ice change occurs on decadal timescales for both $0.5xCO_2$ and $2xCO_2$

Given strong correspondence between zonal-temporal responses of surface temperature (figure 2) and sea ice (figure 3), we next map their spatial evolution (figure 4). We find the largest surface ocean temperature responses at high northern latitudes are associated with sea ice loss or gain. In response to 2xCO₂ forcing, the central Arctic Ocean has large surface warming (figures 4(a) and (b)) and sea ice loss (figures 4(c) and (d)). When compared to the first 150 years (figures 4(a) and (c)), the multi-century 2xCO₂ response (figures 4(b) and (d)) magnitude increases slightly but retains the same response pattern. Under 0.5xCO₂, spatially coherent surface cooling (figures 4(e) and (f)) and sea ice gain (figures 4(g) and (h)) is most pronounced outside of the Arctic Ocean Basin in both the North Pacific and the North Atlantic. On multi-century timescales, this 0.5xCO₂ sea ice gain increases in magnitude and creeps increasingly southward. By the end of the 0.5xCO₂ simulation (years 850–1000, figure 4(h)), sea ice covers the entire Labrador Sea (Southwest of Greenland), the entire Greenland–Iceland–Norwegian Sea (North of Iceland), and much of the Bering Sea (between Russia and Alaska). Interestingly, the largest land surface temperature responses are also spatially adjacent to ocean regions with large sea ice change.

While the high northern latitude surface temperature response is often associated with sea ice change, there are exceptions. First, mid-latitude land surface temperature responses maximize in continental



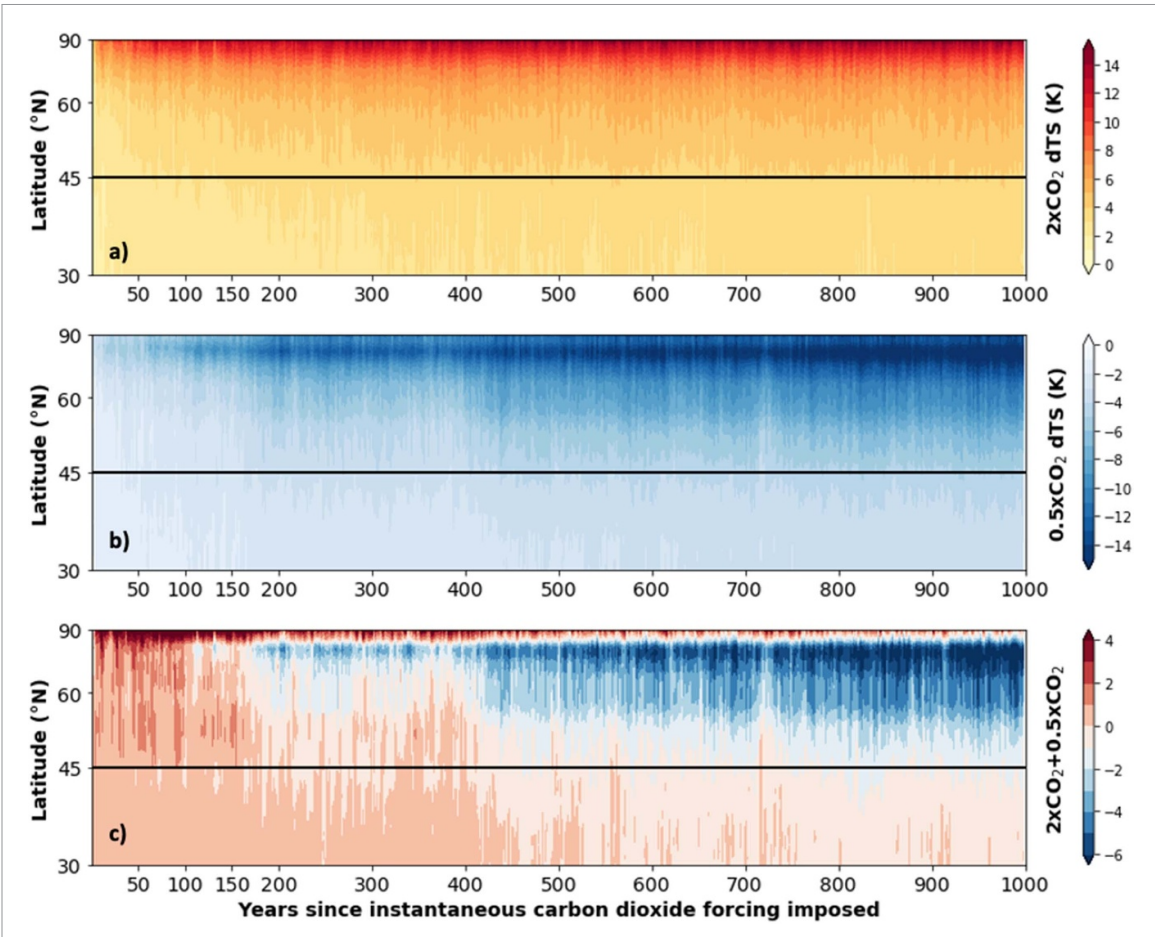


Figure 2. Annual zonal mean surface temperature response (dTS) as a function of year since instantaneous greenhouse forcing applied and northern hemisphere latitude: (a) $2xCO_2$, (b) $0.5xCO_2$, (c) $2xCO_2 + 0.5xCO_2$. For (c)—blue colors indicate a larger change magnitude for $0.5xCO_2$ than for $2xCO_2$ while red colors indicate a larger change magnitude for $2xCO_2$ than for $2xCO_2$. All responses are relative to the 1850 control run years 400-1399 (CNT, see table 1).

interiors under warming (figures 4(a) and (b)). Second, the North Atlantic has opposite-of-global responses that are unassociated with sea ice during the early decades of the simulations. Under $2xCO_2$, a small cooling patch occurs in the first 150 years in the North Atlantic (figure 4(a)) away from the sea ice edge (figure 4(c)). This early cooling region turns to a reduced warming region by year 1000 (figure 4(b)), a sign reversal unexplained by sea ice (figure 4(d)). Under $0.5xCO_2$, a small patch of North Atlantic warming occurs in the first 150 years (figure 4(e)). This early warming hole region reverses sign to become a region of relatively strong cooling by year 1000 (figure 4(f)) coincident with sea ice expansion in the region (figure 4(h)).

The strength of the Atlantic Meridional Overturning Circulation (AMOC) (figure 5) helps explain the time-evolving responses in the North Atlantic. Indeed, AMOC strength is consistent with early opposite-of-global sign temperature responses noted under 2xCO₂ (figure 4(a)) and 0.5xCO₂ (figure 4(e)). Specifically, a weakening of AMOC in the first decades of 2xCO₂ is consistent with the early North Atlantic cooling. Similarly, an early AMOC strengthening is consistent with early North Atlantic cooling under 0.5xCO₂ forcing. After year 150, these early AMOC strength changes decrease and AMOC returns close to its initial strength in the 1850 control run. On multi-century timescales, any initially opposite-of-global surface temperature responses driven by AMOC are overwhelmed by other processes, including especially 0.5xCO₂ sea ice expansion into the North Atlantic on multi-century timescales (figure 4(h)).

3.2. Feedback analysis

Because previous work has found $2xCO_2$ radiative forcing is $\sim 10\%$ larger than $0.5xCO_2$ radiative forcing in CESM1 (see Chalmers et al 2022 table 1), feedbacks differences must explain the larger $0.5xCO_2$ surface cooling than $2xCO_2$ surface warming on multi-century timescales. Indeed, globally averaged feedbacks are less negative for $0.5xCO_2$ than for $2xCO_2$, especially after year 500 (see supplementary figure 1). Averaged over years 850-1000, the global total feedback parameter was $-0.71 \text{ Wm}^{-2}K^{-1}$ for $0.5xCO_2$ and $-0.94 \text{ Wm}^{-2}K^{-1}$ for $2xCO_2$. Here, we are focused on explaining the high northern latitudes. Thus, we next employ radiative feedback analysis to identify which individual feedbacks explain the magnitude and pacing



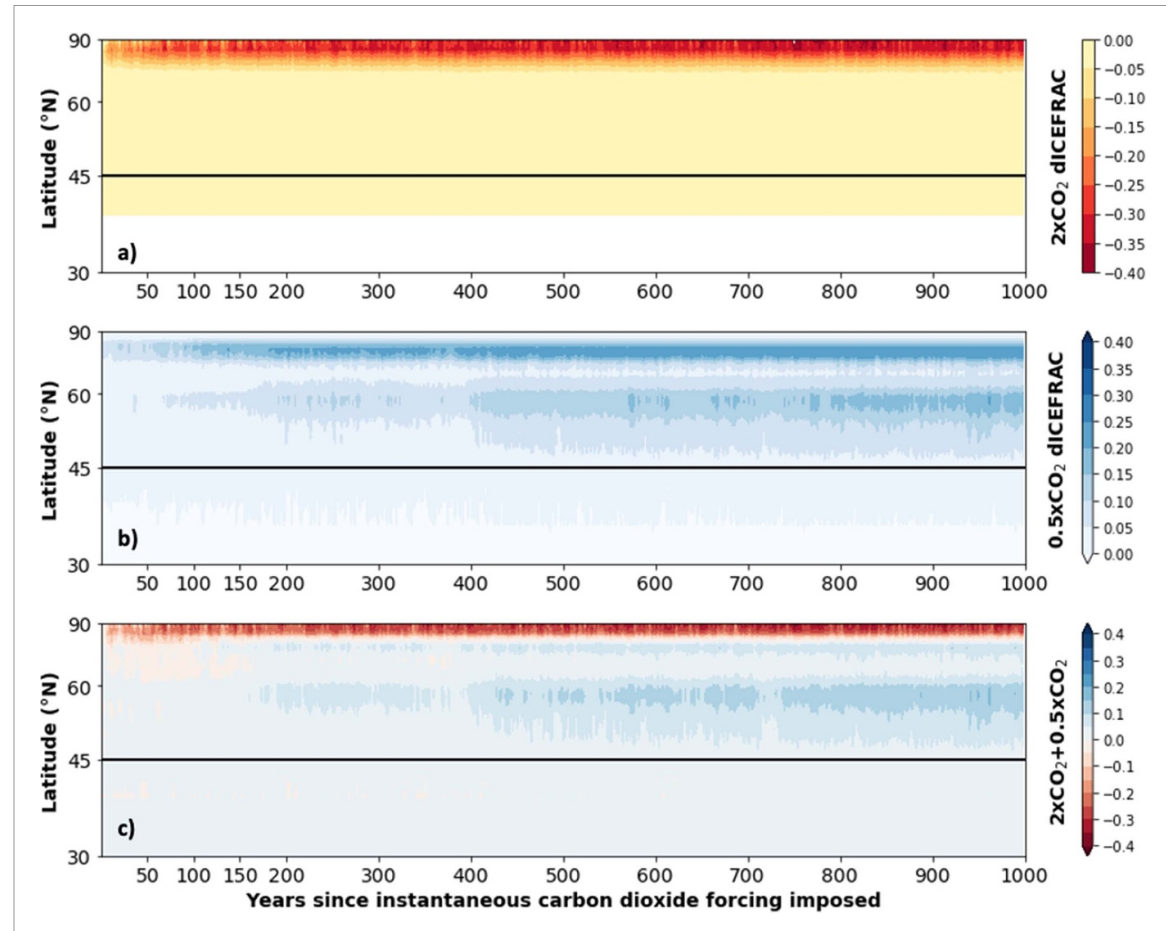


Figure 3. Annual zonal mean sea ice fraction response (dICEFRAC) as a function of year since instantaneous greenhouse forcing applied and northern hemisphere latitude: (a) $2xCO_2$, (b) $0.5xCO_2$, (c) $2xCO_2 + 0.5xCO_2$. For (c)—blue colors indicate a larger change magnitude for $0.5xCO_2$ than for $2xCO_2$ while red colors indicate a larger change magnitude for $2xCO_2$ than for $0.5xCO_2$. All responses are relative to the 1850 control run years 400-1399 (CNT, see table 1).

of the high northern latitude surface temperature responses. We are particularly interested in understanding the time and latitude evolution of individual feedbacks as the surface temperature response shifts poleward under 2xCO₂ forcing and into the mid-latitudes under 0.5xCO₂ forcing.

We next assess individual high-northern latitude feedbacks at the end of the 1000 year long runs (figure 6). At high northern latitudes ($45-90^{\circ}$ N), the positive lapse rate feedback is larger for 0.5xCO_2 forcing than for 2xCO_2 forcing (figure 6(a)). Ocean areas with sea ice, not the land, explain this large lapse rate feedback difference (figure 6(b)). An oceanic origin for this lapse rate difference is also consistent with the location and pacing of the sea ice and surface temperature responses (figure 4). While there is more land at the mid-latitudes of the northern hemisphere, land processes are not the primary drivers of mid-latitude surface temperature response and feedback differences.

Having shown the positive lapse rate feedback over ocean regions is a key driver of high northern mid-latitude cooling on multi-century timescales, we next examine other feedbacks. The cloud, water vapor, and Planck feedbacks all have small magnitudes and/or small differences between $2xCO_2$ warming and $0.5xCO_2$ cooling. Thus, we turn our attention to another large positive feedback associated with sea ice change: the surface albedo feedback. Surprisingly, positive $45-90^\circ$ N surface albedo feedbacks are only slightly larger under $0.5xCO_2$ cooling than under $2xCO_2$ warming (figure 6(a)). Over the oceans (figure 6(b)), the $45-90^\circ$ N surface albedo feedbacks are larger under $2xCO_2$ than under $0.5xCO_2$. A larger surface albedo feedback under $2xCO_2$ than under $0.5xCO_2$ is especially prominent over the highest northern latitude oceans ($70-90^\circ$ N, figures 6(c) and 0).

Given that the lapse rate and surface albedo feedbacks differ the most between $2xCO_2$ warming and $0.5xCO_2$ cooling (figure 5), we assess their zonal time evolution (figure 7). We find the zonal time evolution of both feedbacks (figure 7) are consistent with the zonal time evolution of the surface temperature (figure 2) and sea ice response (figure 3). Under $0.5xCO_2$, the surface albedo and lapse rate feedbacks both increase in strength on multi century timescales at all but the very highest northern latitudes. The time evolution of the lapse rate and surface albedo feedbacks are consistent with continued high northern latitude $0.5xCO_2$



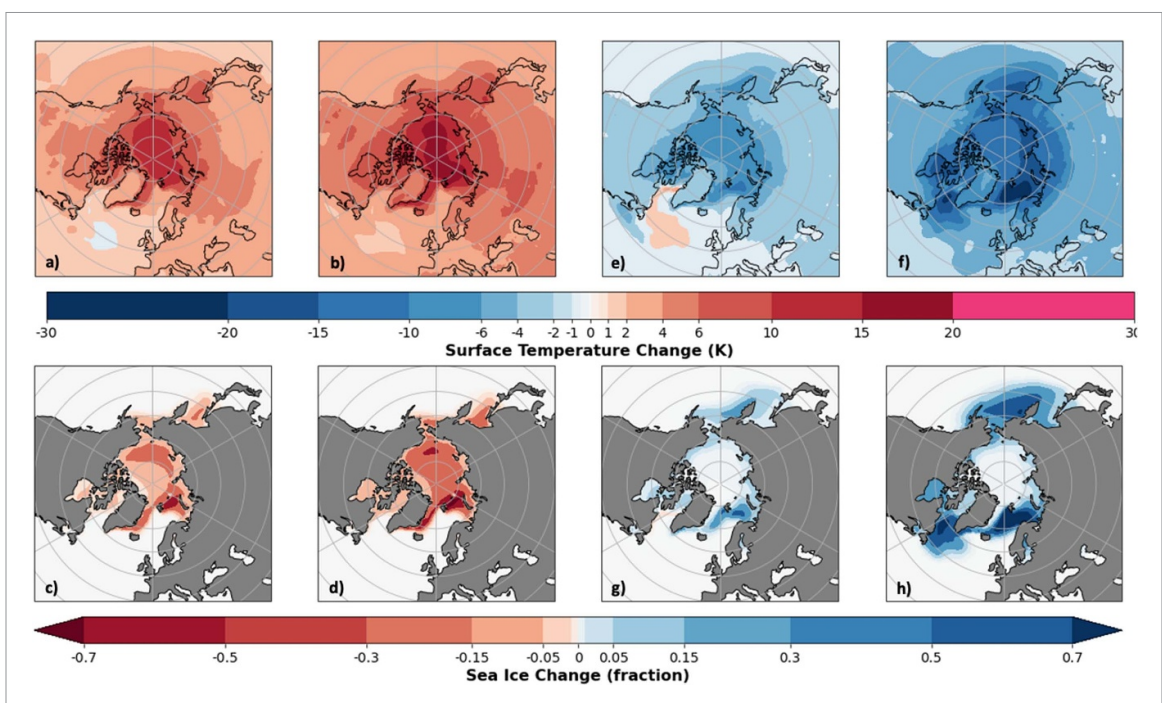


Figure 4. Polar maps of annual high northern latitude response: (a) $2xCO_2$ surface temperature early (years 1–150), (b) $2xCO_2$ surface temperature late (years 850–1000), (c)–(d) as in (a)–(b) but for sea ice, (e) $0.5xCO_2$ surface temperature early, (f) $0.5xCO_2$ surface temperature late, (g)–(h) as in (e)–(f) but for sea ice. All responses are relative to the 1850 control (years 400-1399 CNT, table 1).

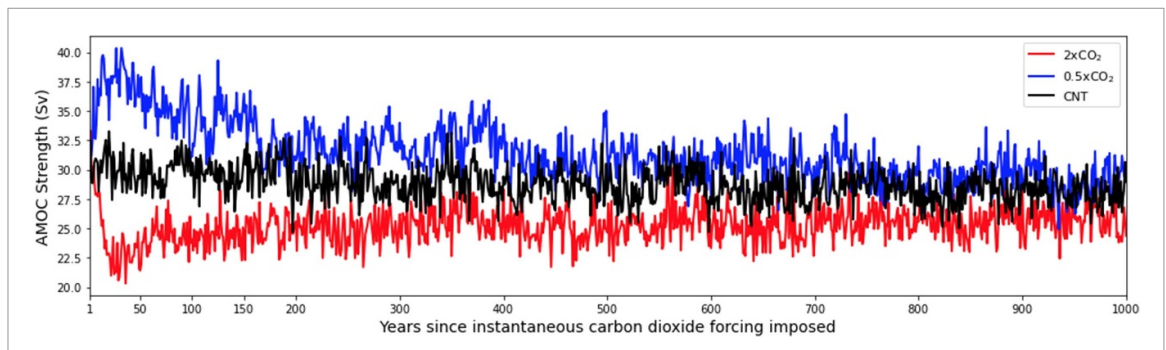


Figure 5. Timeseries of Annual Mean Max Atlantic Meridional Overturning Circulation (AMOC) strength. AMOC strength defined as the maximum meridional overturning in Sverdrups (Sv) in the North Atlantic (30–55 degrees N and 800–2000 meters depth). CNT plotted for years 400–1399.

cooling on multi-century timescales and with fast $2xCO_2$ warming on decadal timescales. Examining these two feedbacks at all latitudes helps justify 45° N latitude for differentiating this high northern latitude sea ice-associated response (i.e. as used in figure 6 and table 1).

4. Discussion

This study addresses a fundamental question: What controls the pacing and magnitude of surface temperature response at high northern latitudes (herein defined as 45–90° N) to idealized greenhouse warming and cooling? Our results based on a modern coupled climate model show that the high northern latitudes respond on decadal timescales for surface greenhouse warming, but on multi-century timescales for surface greenhouse cooling. This finding is consistent with earlier modeling work by Stouffer (2004). While Stouffer (2004) emphasized the importance of ocean vertical mixing for explaining response timescale differences, our results show sea ice change and associated positive feedbacks are also important. Putting these ideas together, sea ice responses in the central Arctic Ocean where vertical mixing is limited are faster than sea ice responses in the mid-latitude oceans. Sea ice and associated positive feedbacks are strongly associated with the timescale and response magnitude differences between greenhouse warming and cooling. In contrast, land processes and the ocean's meridional overturning circulation had a minor influence on our results. The North Atlantic overturning ocean circulation produced a small opposite-of-global surface



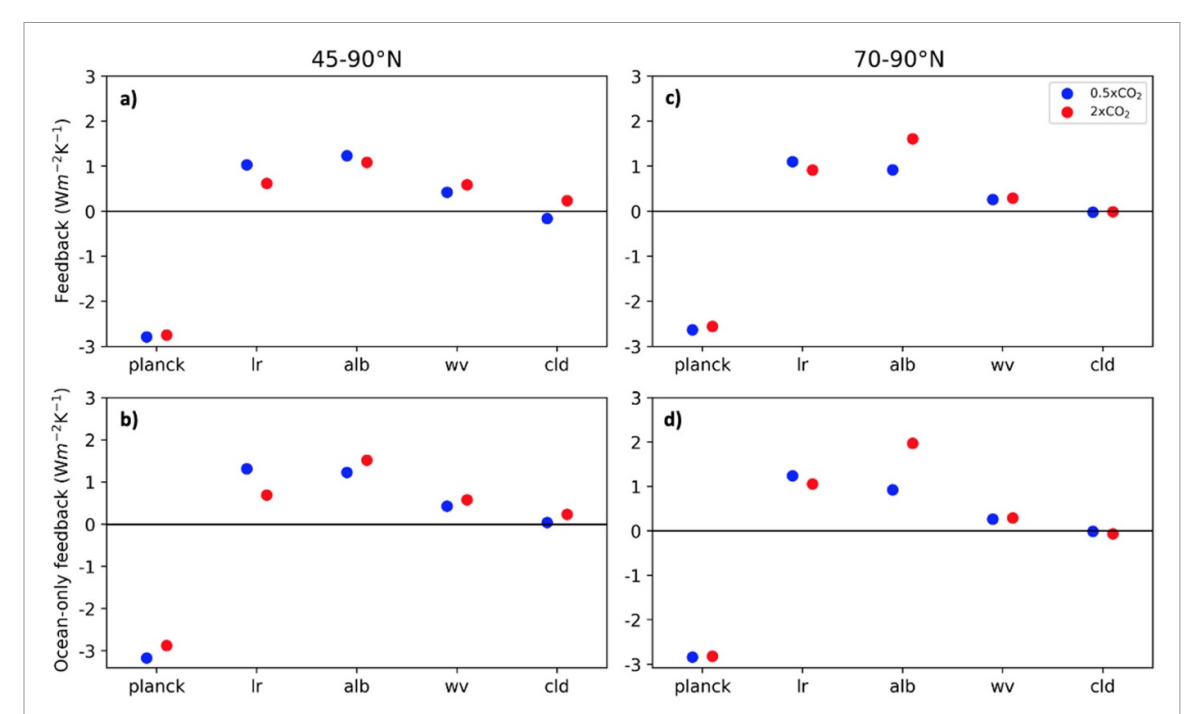


Figure 6. High Northern Hemisphere Radiative Feedback Parameters: (a) $45-90^{\circ}$ N, (b) $70-90^{\circ}$ N, (c)-(d) as in (a)-(b) but for ocean only. Feedback parameters calculated for years 850-999 with CNT years 400-549 as a reference climate for the Planck ('planck'), lapse rate ('lr'), surface albedo ('alb'), water vapor ('wv') and cloud ('cld') feedbacks.

temperature response locally over the first decades. Yet, this early multi-decadal response was overwhelmed on multi-century timescales. Thus, the importance of the North Atlantic overturning for explaining the high northern latitude climate response on multi-century timescale was second-order.

As the mid-latitudes become increasingly cold and sea ice covered, climate feedbacks typically associated with the modern Arctic creep southward. Indeed, this work shows how the sea ice-associated feedbacks that typically amplify modern Arctic climate warming (i.e. the interlinked positive surface-based lapse-rate and positive surface albedo feedbacks) can easily extend into the mid-latitudes and amplify the response to greenhouse gases there. The positive lapse rate feedback is especially important on multi-century timescales for explaining continued 0.5xCO₂ northern mid-latitude cooling. Thus, feedback analysis provides new perspectives on the relative importance of the surface albedo and lapse rate feedbacks beyond their modern latitudinal domain.

That high northern latitude greenhouse cooling is larger but takes longer to emerge than greenhouse warming is consistent with modeling of the Last Glacial Maximum that includes greenhouse gas reductions along with other forcing changes such as ice sheet topography and orbital parameters (e.g. Zhu and Poulsen 2021). This work complements Last Glacial Maximum work using more idealized forcing that enables quantification of the timescales of the processes involved to greenhouse cooling alone. For example, this work finds the processes that amplify greenhouse cooling alone operate on timescales that are double those for amplifying greenhouse warming alone.

While new insights emerged from this work, many additional avenues for research remain. First, our findings show that as the latitude with sea ice present decreases, the lapse rate feedback becomes increasingly dominant and positive. But—what controls the relative strength of the surface albedo and lapse rate feedbacks associated with changing sea ice cover? Related—as the mid-latitudes cool—how does the balance of radiative-advective and radiative-convective processes change? Analyzing the analytical model of Feldl and Merlis (2023) could provide interesting insights to this question. Second, the robustness of these findings and their underlying physical mechanisms should be further assessed. More could be done to understand the ocean processes setting the timescales and location of sea ice expansion at northern mid-latitudes. Given that global cooling and sea ice expansion modifies boundary layer moisture budgets and cloud processes, additional investigation of cloud influence on global cooling also remains an interesting and open research area. While cloud feedbacks were not found to be a dominant process in explaining the responses in this work, this finding did not surprise us. While CESM1 can replicate observed cloud sea ice relationships (Morrison et al 2019), CESM1 has insufficient supercooled liquid in the clouds and thus the strength of extratropical cloud feedbacks and cloud masking are not reliable (e.g. Kay et al 2016, Tan et al 2016, Middlemas et al 2020). Care needs to be taken to not overinterpret model results when a known model



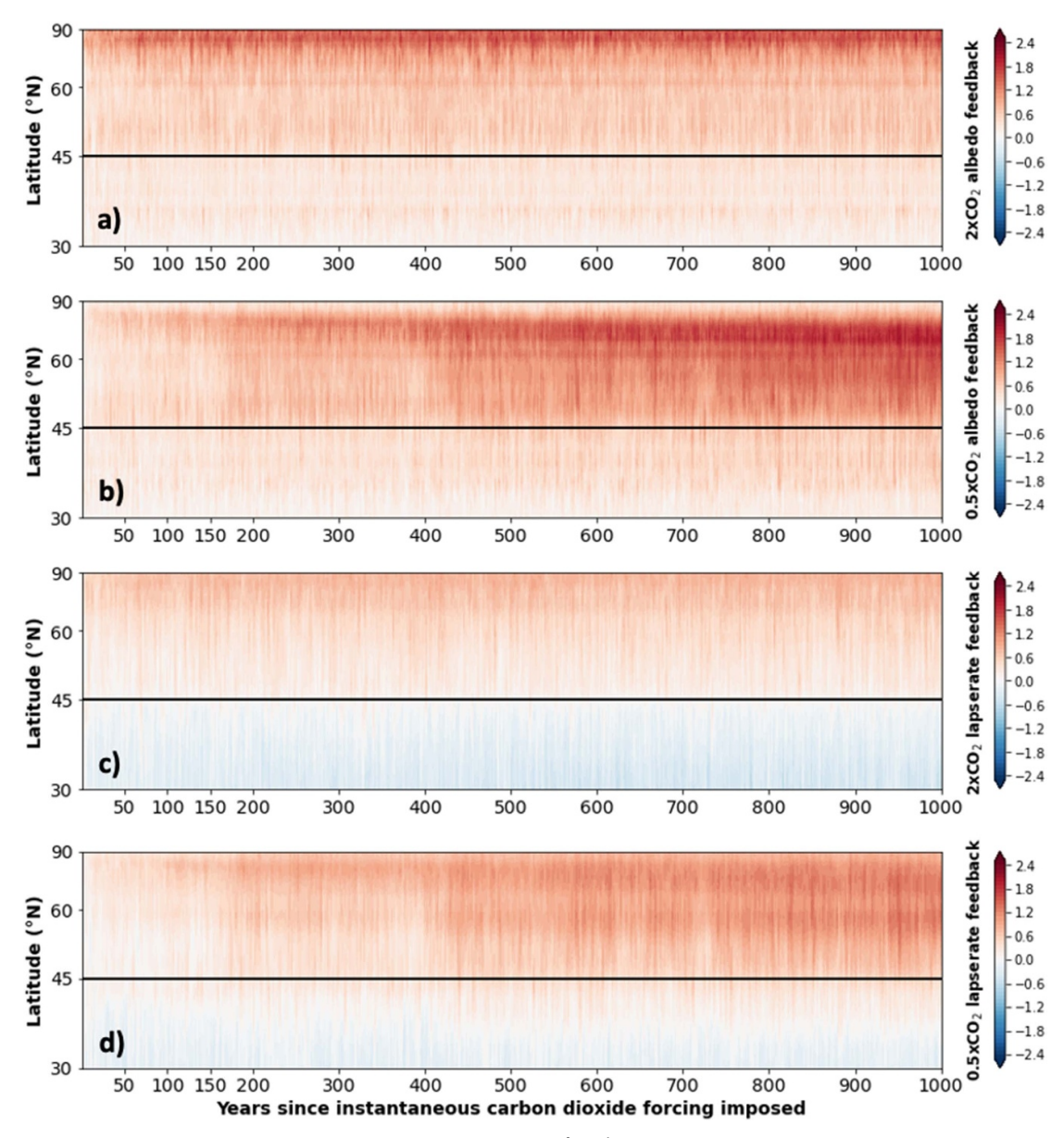


Figure 7. Zonal-mean time evolution of feedback parameters (Wm $^{-2}$ K $^{-1}$): (a) 2xCO $_2$ surface albedo feedback, (b) 0.5xCO $_2$ surface albedo feedback, (c) 2xCO $_2$ lapse rate feedback, (d) 0.5xCO $_2$ lapse rate feedback. Feedback parameters calculated with CNT years 400–549 as a reference climate.

limitation could fundamentally affect the outcome. While the greenhouse cooling model experiment analyzed in this work is 1000 years long, this simulation has not reached equilibrium and would likely continue to cool given more years of integration. Finally, the influence of land ice retreat or expansion is not included in this work, could be important, and remains to be addressed by future work.

5. Summary

We use a modern global coupled climate model to assess the processes controlling the pacing and magnitude of the high northern latitude response to greenhouse warming and cooling. In contrast to rapid greenhouse warming and sea ice loss on multi-decadal timescales at the highest northern latitudes, greenhouse cooling in the mid-latitudes results from sea ice expansion equatorward and associated positive feedbacks on multi-century timescales. Future work should continue to probe the processes controlling responses on multi-century timescales as resources allow, as these processes are less studied especially for greenhouse cooling. More broadly, this work shows the value of idealized model experiments in a modern global climate model used for future climate projections to probe the processes underlying cooling and warming response asymmetries in the climate system.



Data availability statement

The full climate model data used in this study are available on National Center for Atmospheric Research Glade Globus Collection at /glade/campaign/univ/ucub0090/longCO2runs. Data for all fields plotted in the paper are available at https://zenodo.org/doi/10.5281/zenodo.10982805.

Acknowledgment

J E K and N M were supported by NSF CAREER award 1554659. J E K further acknowledges support from NSF award OPP 2233420. N M further acknowledges support from Australian Research Council Centre of Excellence for Climate Extremes (CE170100023). Y L and S Z are supported by grants from the National Science and Technology Council (112-2628-M-002-009 and 113-2628-M-002-018) to National Taiwan University. All authors acknowledge fruitful discussion about this work with Ivan Mitevski, Lorenzo Polvani, Jiang Zhu, Jonah Shaw, Yue Dong, and Elizabeth Maroon. In addition, we acknowledge high-performance computing support from Cheyenne (doi:10.5065/D6RX99HX) provided by NCAR's Computational and Information Systems Laboratory, sponsored by the National Science Foundation.

Conflict of interest

The authors have no conflicts of interest to report.

ORCID iDs

Jennifer E Kay https://orcid.org/0000-0002-3625-5377 Yu-Chiao Liang https://orcid.org/0000-0002-9347-2466 Shih-Ni Zhou https://orcid.org/0009-0006-1739-751X Nicola Maher https://orcid.org/0000-0003-3922-9833

References

Armour K C, Bitz C M and Roe G H 2013 Time-varying climate sensitivity from regional feedbacks *J. Clim.* 26 4518–34 Chalmers J, Kay J E, Middlemas E A, Maroon E A and DiNezio P 2022 Does disabling cloud radiative feedbacks change spatial patterns of surface greenhouse warming and cooling? *J. Clim.* 35 1787–807

Eyring V, Bony S, Meehl G A, Senior C A, Stevens B, Stouffer R J and Taylor K E 2016 Overview of the coupled model intercomparison project phase 6 (CMIP6) experimental design and organization *Geosci. Model Dev.* 9 1937–58

Feldl N and Merlis T M 2023 A semi-analytical model for water vapor, temperature, and surface-albedo feedbacks in comprehensive climate models *Geophys. Res. Lett.* **50** e2023GL105796

Frey W R and Kay J E 2017 The influence of extratropical cloud phase and amount feedbacks on climate sensitivity *Clim. Dyn.* **50** 3097–116

Hill S A, Burls N J, Fedorov A and Merlis T M 2022 Symmetric and antisymmetric components of polar-amplified warming *J. Clim.* 35 3157–72

Hurrell J *et al* 2013 The community earth system model: a framework for collaborative research *Bull. Am. Meteorol. Soc.* **94** 1339–60 Jansen M F, Nadeau L-P and Merlis T M 2018 Transient versus equilibrium response of the ocean's overturning circulation to warming *J. Clim.* **31** 5147–63

Kay J E et al 2015 The community Earth system model (CESM) large ensemble project: a community resource for studying climate change in the presence of internal climate variability Bull. Am. Meteorol. Soc. 96 1333–49

Kay J E, Bourdages L, Chepfer H, Miller N, Morrison A, Yettella V and Eaton B 2016 Evaluating and improving cloud phase in the community atmosphere model version 5 using spaceborne lidar observations J. Geophys. Res. 121 4162–76

Knutti R, Masson D and Gettelman A 2013 Climate model genealogy: generation CMIP5 and how we got there Geophys. Res. Lett. 40 1194–9

Kutzbach J E, He F, Vavrus S J and Ruddiman W F 2013 The dependence of equilibrium climate sensitivity on climate state: applications to studies of climates colder than present *Geophys. Res. Lett.* 40 3721–6

Manabe S, Stouffer R J, Spelman M J and Bryan K 1991 Transient response of a coupled ocean–atmosphere model to gradual changes of atmospheric CO₂. Part I: annual-mean response *J. Clim.* 4 785–818

Middlemas E A, Kay J E, Medeiros B M and Maroon E A 2020 Quantifying the influence of cloud radiative feedbacks on Arctic surface warming using cloud locking in an earth system model *Geophys. Res. Lett.* 47 e2020GL089207

Mitevski I, Orbe C, Chemke R, Nazarenko L and Polvani L M 2021 Non-monotonic response of the climate system to abrupt CO₂ forcing Geophys. Res. Lett. 48 e2020GL090861

Mitevski I, Polvani L M and Orbe C 2022 Asymmetric warming/cooling response to CO₂ increase/decrease mainly due to non-logarithmic forcing, not feedbacks *Geophys. Res. Lett.* 49 e2021GL097133

Morrison A L, Kay J E, Frey W R, Chepfer H and Guzman R 2019 Cloud response to Arctic sea ice loss and implications for future feedbacks in the CESM1 climate model *J. Geophys. Res.* 124 1003–20

Pendergrass A, Conley A and Vitt F M 2018 Surface and top-of-atmosphere radiative feedback kernels for CESM-CAM5 Earth Syst. Sci. Data 10 317–24

Rugenstein M A et al 2020 Equilibrium climate sensitivity estimated by equilibrating climate models Geophys. Res. Lett. 47 e2019GL083898



Rugenstein M et al 2019 LongRunMIP—motivation and design for a large collection of millennial-length GCM simulations Bull. Am. Meteorol. Soc. 100 2551–70

Sherwood S *et al* 2020 An assessment of Earth's climate sensitivity using multiple lines of evidence *Rev. Geophys.* **58** e2019RG000678 Stouffer R J 2004 Time scales of climate response *J. Clim.* **17** 209–17

Stouffer R and Manabe S 2003 Equilibrium response of thermohaline circulation to large changes in atmospheric CO₂ concentration Clim. Dyn. 20 759–73

Tan I, Storelvmo T and Zelinka M D 2016 Observational constraints on mixed-phase clouds imply higher climate sensitivity *Science* 352 224–7

Yang H and Zhu J 2011 Equilibrium thermal response timescale of global oceans Geophys. Res. Lett. 38

Zhou S-N, Liang Y-C, Mitevski I and Polvani L 2023 Stronger Arctic amplification produced by decreasing, not increasing, CO₂ concentrations *Environ. Res.* 2 045001

Zhu J, Otto-Bliesner B L, Brady E C, Gettelman A, Bacmeister J T, Neale R B, Poulsen C J, Shaw J K, McGraw Z S and Kay J E 2022 LGM paleoclimate constraints inform cloud parameterizations and equilibrium climate sensitivity in CESM2 *J. Adv. Model. Earth Syst.* 14 e2021MS002776

Zhu J and Poulsen C J 2021 Last glacial maximum (LGM) climate forcing and ocean dynamical feedback and their implications for estimating climate sensitivity Clim. Past 17 253–67